SUPPLEMENTARY INFORMATION

Evoking picomolar binding in RNA by a single phosphorodithioate linkage

N. Dinuka Abeydeera,[1] Martin Egli,[2,*] Nehemiah Cox,[3] Karen Mercier,[4] Jonas Nascimento Conde,[5] Pradeep S. Pallan,[2] Daniella M. Mizurini,[6] Malgorzata Sierant,[7] Fatima-Ezzahra Hibti,[4] Tom Hassell,[8] Tianzhi Wang,[9] Feng-Wu Liu,[10] Hong-Min Liu,[10] Carlos Martinez,[8] Anil K. Sood,[11] Terry P. Lybrand,[12] Chiraz Frydman,[4] Robson Q. Monteiro,[6] Richard H. Gomer,[3] Barbara Nawrot,[7] Xianbin Yang[1,*]

[1]AM Biotechnologies, LLC, 12521 Gulf Freeway, Houston, Texas 77034, USA

[2]Department of Biochemistry, Vanderbilt University, School of Medicine, Nashville, TN 37232, USA

[3]Department of Biology, Texas A&M University, College Station, TX 77843, USA

[4]Biointeractions Division, Horiba Scientific, Avenue de la Vauve - Passage JobinYvon CS 45002 Palaiseau, France

[5]Instituto de Biofísica Carlos Chagas Filho, Federal University of Rio de Janeiro, Rio de Janeiro, RJ 21941, Brazil

[6]Instituto de Bioquimica Médica Leopoldo de Meis, Federal University of Rio de Janeiro, Rio de Janeiro, RJ 21941, Brazil

[7]Department of Bioorganic Chemistry, Centre of Molecular and Macromolecular Studies, Polish Academy of Sciences, 90-363 Lodz, Sienkiewicza 112, Poland

[8]Sigma Life Science, 9186 Six Pines, The Woodlands, Texas 77380, USA

[9]The Sealy Center for Structural Biology & Molecular Biophysics, University of Texas Medical Branch, Galveston, Texas 77555, USA

[10]School of Pharmaceutical Sciences, Zhengzhou University, Science Avenue 100, Zhengzhou 450001, Henan, China

[11]Departments of Gynecologic Oncology and Cancer Biology, and Center for RNAi and Non-coding RNA, The University of Texas MD Anderson Cancer Center, Houston, Texas 77054, USA

[12]Departments of Chemistry and Pharmacology, and Center for Structural Biology, Vanderbilt University, Nashville, TN 37232, USA

Supplementary Table 1 (ST-1): The library of candidate aptamer sequences for $VEGF_{165}$. Each RNA sequence (AF83-1 and AF83-2 to AF83-23) is labeled with biotin at the 5′-end using the Biotin-TEG phosphoramidite (Glen Research). AF83-1 is the known aptamer sequence that binds to $VEGF_{165}$. The sequences, AF83-2 to AF83-23 are synthesized by systematically substituting PS2 onto each residue (red). All nucleotides except for T are substituted with a 2′-OMe.

Name	Sequence information
AF83-1	5'-Biotin-AUG CAG UUU GAG AAG UCG CGC AUT-3'
AF83-2	5'-Biotin-A_{PS2}UG CAG UUU GAG AAG UCG CGC AUT-3'
AF83-3	5'-Biotin-AU_{PS2}G CAG UUU GAG AAG UCG CGC AUT-3'
AF83-4	5'-Biotin-AUG_{PS2} CAG UUU GAG AAG UCG CGC AUT-3'
AF83-5	5'-Biotin-AUG C_{PS2}AG UUU GAG AAG UCG CGC AUT-3'
AF83-6	5'-Biotin-AUG CA_{PS2}G UUU GAG AAG UCG CGC AUT-3'
AF83-7	5'-Biotin-AUG CAG_{PS2} UUU GAG AAG UCG CGC AUT-3'
AF83-8	5'-Biotin-AUG CAG U_{PS2}UU GAG AAG UCG CGC AUT-3'
AF83-9	5'-Biotin-AUG CAG UU_{PS2}U GAG AAG UCG CGC AUT-3'
AF83-10	5'-Biotin-AUG CAG UUU_{PS2} GAG AAG UCG CGC AUT-3'
AF83-11	5'-Biotin-AUG CAG UUU G_{PS2}AG AAG UCG CGC AUT-3'
AF83-12	5'-Biotin-AUG CAG UUU GA_{PS2}G AAG UCG CGC AUT-3'
AF83-13	5'-Biotin-AUG CAG UUU GAG_{PS2} AAG UCG CGC AUT-3'
AF83-14	5'-Biotin-AUG CAG UUU GAG A_{PS2}AG UCG CGC AUT-3'
AF83-15	5'-Biotin-AUG CAG UUU GAG AA_{PS2}G UCG CGC AUT-3'
AF83-16	5'-Biotin-AUG CAG UUU GAG AAG_{PS2} UCG CGC AUT-3'
AF83-17	5'-Biotin-AUG CAG UUU GAG AAG U_{PS2}CG CGC AUT-3'
AF83-18	5'-Biotin-AUG CAG UUU GAG AAG UC_{PS2}G CGC AUT-3'
AF83-19	5'-Biotin-AUG CAG UUU GAG AAG UCG_{PS2} CGC AUT-3'
AF83-20	5'-Biotin-AUG CAG UUU GAG AAG UCG C_{PS2}GC AUT-3'
AF83-21	5'-Biotin-AUG CAG UUU GAG AAG UCG CG_{PS2}C AUT-3'
AF83-22	5'-Biotin-AUG CAG UUU GAG AAG UCG CGC_{PS2} AUT-3'
AF83-23	5'-Biotin-AUG CAG UUU GAG AAG UCG CGC A_{PS2}UT-3'

Supplementary Table 2 (ST-2): The library of candidate aptamer sequences with PS2 substitutions for α-thrombin. Each RNA sequence (AF113-1 and AF113-2 to AF113-25) is labeled with biotin at the 5′-end using the Biotin-TEG phosphoramidite (Glen Research). AF113-1 is the known aptamer sequence that binds to human α-Thrombin. The sequences, AF113-2 to AF113-25 are synthesized by systematically substituting PS2 onto each residue (red). All Cs and Us are 2′-fluoro-ribounits.

Name	Sequence information
AF113-1	5'-Biotin-GGGAACAAAGCUGAAGUACUUACCCT-3'
AF113-2	5'-Biotin-G_{PS2}GGAACAAAGCUGAAGUACUUACCCT-3'
AF113-3	5'-Biotin-GG_{PS2}GAACAAAGCUGAAGUACUUACCCT-3'
AF113-4	5'-Biotin-GGG_{PS2}AACAAAGCUGAAGUACUUACCCT-3'
AF113-5	5'-Biotin-GGGA_{PS2}ACAAAGCUGAAGUACUUACCCT-3'
AF113-6	5'-Biotin-GGGAA_{PS2}CAAAGCUGAAGUACUUACCCT-3'
AF113-7	5'-Biotin-GGGAAC_{PS2}AAAGCUGAAGUACUUACCCT-3'
AF113-8	5'-Biotin-GGGAACA_{PS2}AAGCUGAAGUACUUACCCT-3'
AF113-9	5'-Biotin-GGGAACAA_{PS2}AGCUGAAGUACUUACCCT-3'
AF113-10	5'-Biotin-GGGAACAAA_{PS2}GCUGAAGUACUUACCCT-3'
AF113-11	5'-Biotin-GGGAACAAAG_{PS2}CUGAAGUACUUACCCT-3'
AF113-12	5'-Biotin-GGGAACAAAGC_{PS2}UGAAGUACUUACCCT-3'
AF113-13	5'-Biotin-GGGAACAAAGCU_{PS2}GAAGUACUUACCCT-3'
AF113-14	5'-Biotin-GGGAACAAAGCUG_{PS2}AAGUACUUACCCT-3'
AF113-15	5'-Biotin-GGGAACAAAGCUGA_{PS2}AGUACUUACCCT-3'
AF113-16	5'-Biotin-GGGAACAAAGCUGAA_{PS2}GUACUUACCCT-3'
AF113-17	5'-Biotin-GGGAACAAAGCUGAAG_{PS2}UACUUACCCT-3'
AF113-18	5'-Biotin-GGGAACAAAGCUGAAGU_{PS2}ACUUACCCT-3'
AF113-19	5'-Biotin-GGGAACAAAGCUGAAGUA_{PS2}CUUACCCT-3'
AF113-20	5'-Biotin-GGGAACAAAGCUGAAGUAC_{PS2}UUACCCT-3'
AF113-21	5'-Biotin-GGGAACAAAGCUGAAGUACU_{PS2}UACCCT-3'
AF113-22	5'-Biotin-GGGAACAAAGCUGAAGUACUU_{PS2}ACCCT-3'
AF113-23	5'-Biotin-GGGAACAAAGCUGAAGUACUUA_{PS2}CCCT-3'
AF113-24	5'-Biotin-GGGAACAAAGCUGAAGUACUUAC_{PS2}CCT-3'
AF113-25	5'-Biotin-GGGAACAAAGCUGAAGUACUUACC_{PS2}CT-3'

Supplementary Figure 1 (SF-1): BLI analysis of anti-VEGF$_{165}$ aptamer sequences. The sequences used in this analysis are shown in **ST-1** and the kinetic parameters corresponding to the global fits are given in **Supplementary Table 3 (ST-3)**. Association was monitored for 300 sec and the dissociation was followed for 300 sec on a FortéBio Octet Red 96 instrument. The data were fit to a 1:1 binding model using FortéBio Octet data analysis software.

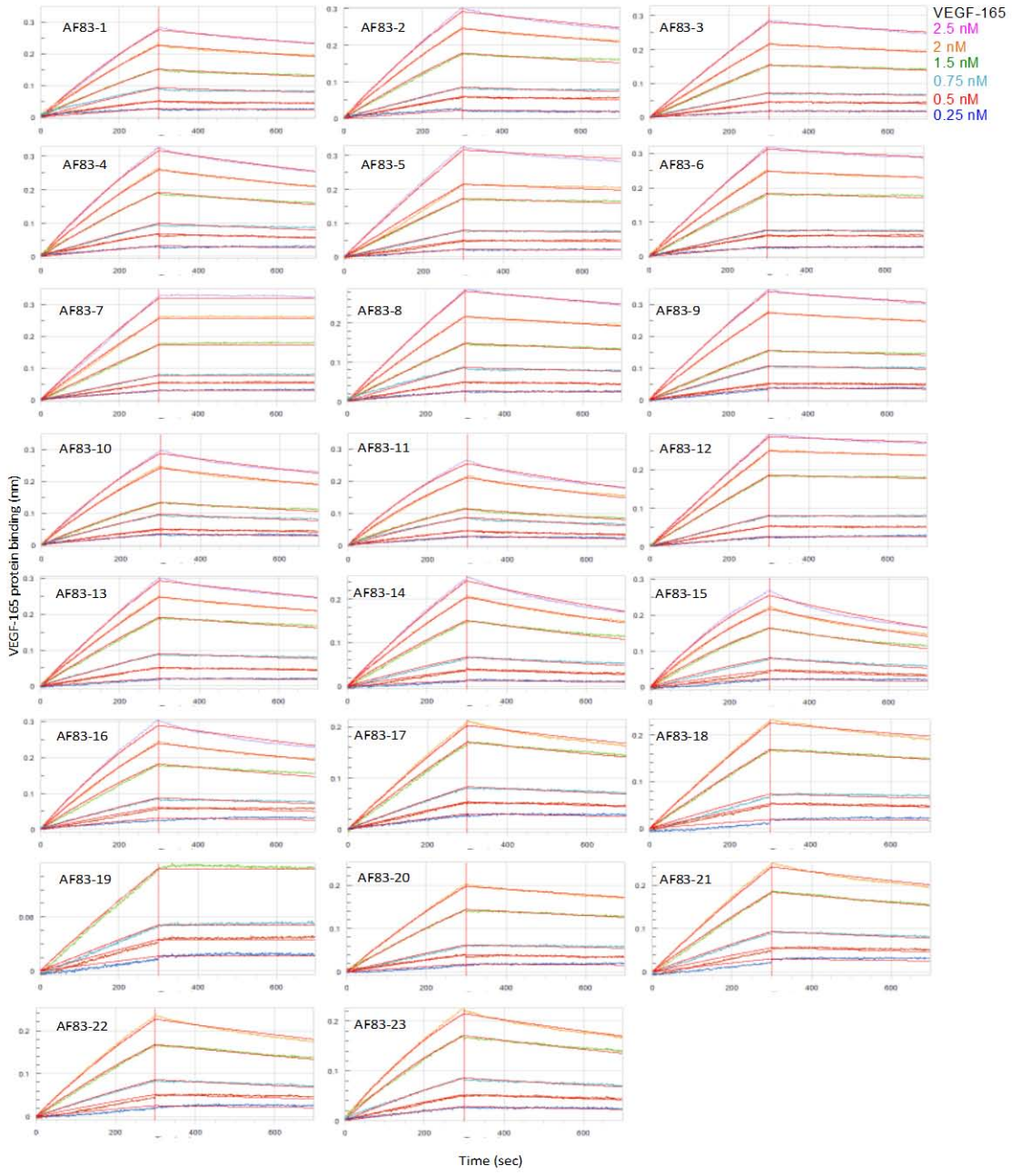

Supplementary Table 3 (ST-3): Affinity ranking of candidate aptamer sequences for $VEGF_{165}$. A stock of 50.0 nM $VEGF_{165}$ in PBST buffer (10 mM Sodium phosphate, 150 mM NaCl, 0.04% Tween 20, pH 7.4) was prepared as a dilution series (0, 1.0, 2.0, 3.0, 4.0, 6.0 nM). Association was monitored for 300 sec and the dissociation was followed for 300 sec on a FortéBIO Octet Red 96 instrument. The dissociation was stretched to at least 1,000 sec to verify tight binding. The data were fit to a 1:1 binding model using fortéBIO Octet data analysis software. Kinetic constants were determined by integration of the experimental data using the differential rate equation $dR/dt = k_{on} \cdot C \cdot (R_{max}-R) - k_{off} \cdot R$ to obtain both the k_a and k_d values (R = observed response, R_{max} =maximum response upon saturation, C = analyte concentration, k_{on} = association rate constant, k_{off} =dissociation rate constant). The ratio between k_{off} and k_{on} corresponds to the reported dissociation constants ($k_{off}/k_{on}=K_D$). The goodness of the global fits was judged by the reduced χ^2 and R^2 values. Relative K_D values are obtained as the ratio of K_D of the unmodified RNA and that of the PS2-modified one (Relative $K_D = K_D^{unsubstituted}/K_D^{substituted}$). Reported K_D values are expressed as mean ± SEM, n = 3.

Name	K_D (pM)	k_{on}(1/Ms)	k_{on} Error	k_{dis}(1/s)	k_{dis} Error	Full χ^2	Full R^2	Relative K_D
AF83-1	**961 ± 25**	4.56E+05	1.12E+04	4.38E-04	3.49E-06	0.049151	0.998215	**1.0**
AF83-2	**982 ± 25**	4.11E+05	1.02E+04	4.04E-04	3.15E-06	0.047172	0.998582	**1.0**
AF83-3	**2665 ± 166**	1.04E+05	6.43E+03	2.77E-04	2.03E-06	0.01702	0.999455	**0.4**
AF83-4	**1012 ± 17**	5.42E+05	8.78E+03	5.49E-04	2.74E-06	0.039834	0.998876	**0.9**
AF83-5	**1675 ± 170**	1.27E+05	1.27E+04	2.13E-04	3.99E-06	0.079093	0.997905	**0.6**
AF83-6	**644 ± 20**	2.86E+05	8.13E+03	1.85E-04	2.49E-06	0.034333	0.999125	**1.5**
AF83-7	**1 ± 0.1**	3.55E+05	1.33E+04	3.6E-07	1.00E-07	0.095737	0.997931	**961.0**
AF83-8	**1557 ± 59**	1.97E+05	7.30E+03	3.07E-04	2.29E-06	0.021537	0.999247	**0.6**
AF83-9	**846 ± 21**	3.05E+05	7.11E+03	2.58E-04	2.22E-06	0.030194	0.999323	**1.1**
AF83-10	**1122 ± 21**	5.48E+05	9.92E+03	6.15E-04	3.18E-06	0.040653	0.998576	**0.9**
AF83-11	**1190 ± 19**	7.56E+05	1.16E+04	8.99E-04	3.81E-06	0.04061	0.998033	**0.8**
AF83-12	**1350 ± 92**	8.97E+04	5.95E+03	1.21E-04	1.80E-06	0.016874	0.999541	**0.7**
AF83-13	**1679 ± 54**	2.56E+05	8.12E+03	4.29E-04	2.53E-06	0.031032	0.999106	**0.6**
AF83-14	**6797 ± 663**	1.27E+05	1.23E+04	8.60E-04	4.14E-06	0.0468	0.997866	**0.1**
AF83-15	**1437 ± 35**	7.56E+05	1.78E+04	1.09E-03	5.86E-06	0.099617	0.995544	**0.7**
AF83-16	**970 ± 26**	5.62E+05	1.46E+04	5.45E-04	4.53E-06	0.09212	0.996973	**1.0**
AF83-17	**3231 ± 352**	1.48E+05	1.61E+04	4.79E-04	4.11E-06	0.027734	0.997862	**0.3**
AF83-18	**2518 ± 444**	1.35E+05	2.37E+04	3.40E-04	6.12E-06	0.070002	0.995958	**0.4**
AF83-19	**1 ± 0.1**	3.99E+05	4.39E+04	4.01E-07	1.05E-07	0.099002	0.993944	**961.0**
AF83-20	**788 ± 28**	4.33E+05	1.44E+04	3.42E-04	3.70E-06	0.019173	0.998512	**1.2**
AF83-21	**4019 ± 838**	1.16E+05	2.41E+04	4.65E-04	6.25E-06	0.08378	0.995481	**0.2**
AF83-22	**1478 ± 86**	3.93E+05	2.24E+04	5.80E-04	5.86E-06	0.060789	0.996065	**0.7**
AF83-23	**572 ± 9**	1.03E+06	1.54E+04	5.89E-04	3.85E-06	0.025495	0.998165	**1.7**

Supplementary Figure (SF-2): BLI analysis of anti-α-thrombin aptamer sequences containing PS2 substitutions. The sequences used in this analysis are shown in **ST-2** and the kinetic parameters corresponding to the global fits are given in **ST-4**. Association was monitored for 300 sec and the dissociation was followed for 300 sec on a FortéBio Octet Red 96 instrument. The data were fit to a 1:1 binding model using FortéBio Octet data analysis software.

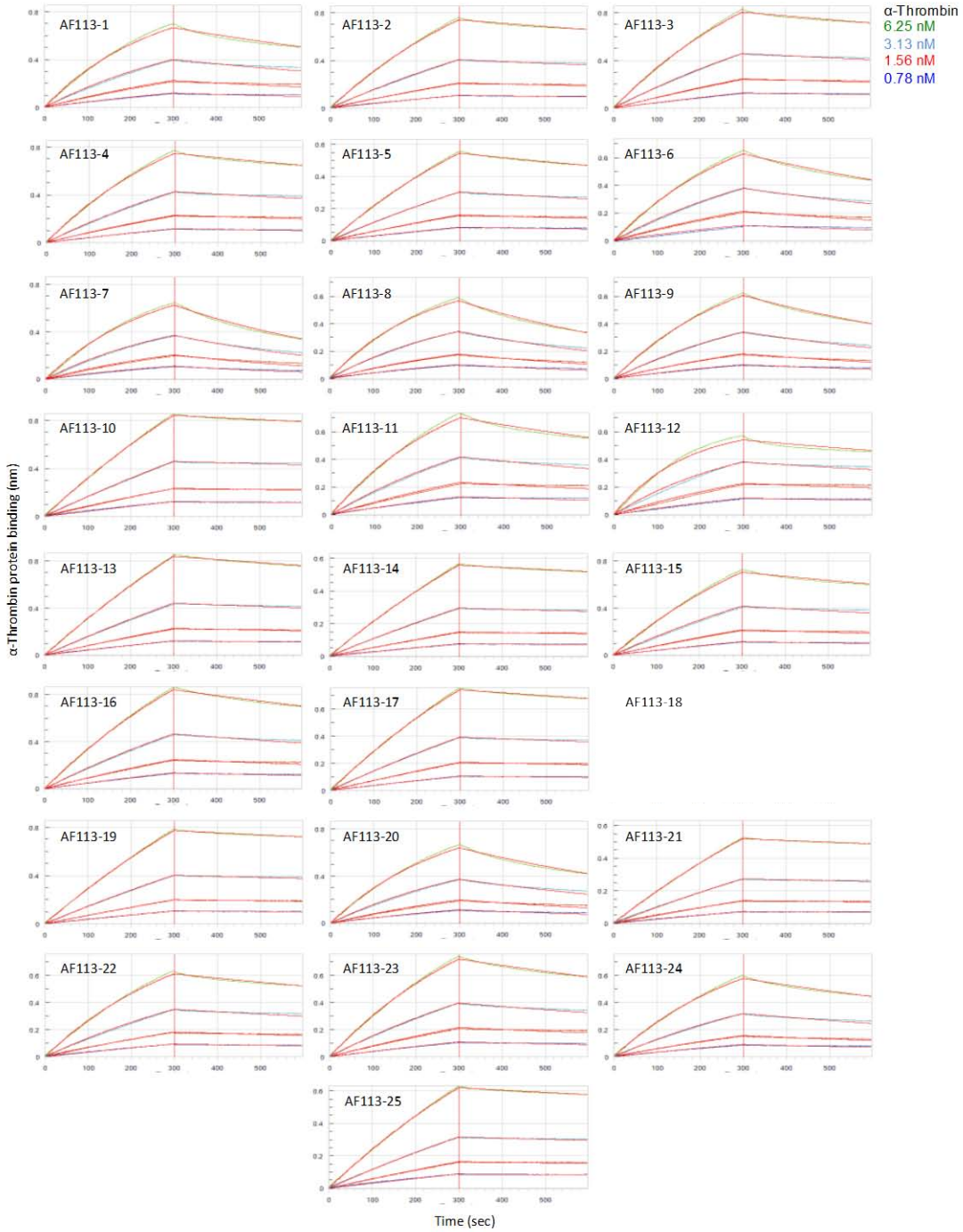

Supplementary Table 4 (ST-4): Affinity ranking of candidate aptamer sequences (with PS2 substitutions) for α-thrombin. A stock of 50.0 nM α-thrombin in HSCT buffer (20 mM HEPES-KOH, 75 mM NaCl,2mM $CaCl_2$, 0.05% Tween 20, pH 7.4) was prepared as a dilution series (0, 1.0, 2.0, 3.0, 4.0, 6.0 nM). Association was monitored for 300 sec and the dissociation was followed for 300 sec on a FortéBio Octet Red 96 instrument. The dissociation was stretched to at least 1,000 sec to verify tight binding. The data were fit to a 1:1 binding model using FortéBio Octet data analysis software. Kinetic constants were determined by integration of the experimental data using the differential rate equation $dR/dt = k_{on} \cdot C \cdot (R_{max}-R) - k_{off} \cdot R$ to obtain both the k_a and k_d values (R = observed response, R_{max} =maximum response upon saturation, C = analyte concentration, k_{on} = association rate constant, k_{off} =dissociation rate constant). The ratio between k_{off} and k_{on} corresponds to the reported dissociation constants ($k_{off}/k_{on}=K_D$). The goodness of the global fits was judged by the reduced χ^2 and R^2 values. Relative K_D values are obtained as the ratio of K_D of the unmodified RNA and that of the PS2-modified one (Relative $K_D = K_D^{unsubstituted}/K_D^{substituted}$). Reported K_D values are expressed as mean ± SEM, n = 3.

Name	K_D (pM)	k_{on}(1/Ms)	k_{on} Error	k_{dis}(1/s)	k_{dis} Error	Full χ^2	Full R^2	Relative K_D
AF113-1	**1871 ± 36**	2.86E+05	4.73E+03	5.34E-04	5.11E-06	0.068668	0.998796	**1.0**
AF113-2	**1260 ± 19**	3.09E+05	3.49E+03	3.90E-04	3.72E-06	0.074347	0.999361	**1.5**
AF113-3	**1225 ± 18**	3.26E+05	3.59E+03	4.00E-04	3.77E-06	0.093047	0.999316	**1.5**
AF113-4	**1287 ± 21**	3.78E+05	4.77E+03	4.86E-04	4.99E-06	0.138395	0.998807	**1.5**
AF113-5	**2229 ± 37**	2.27E+05	3.35E+03	5.05E-04	3.63E-06	0.037701	0.999379	**0.8**
AF113-6	**3784 ± 90**	3.17E+05	7.25E+03	1.20E-03	8.00E-06	0.217207	0.996952	**0.5**
AF113-7	**6475 ± 168**	3.16E+05	8.07E+03	2.04E-03	9.56E-06	0.239535	0.996176	**0.3**
AF113-8	**4030 ± 63**	4.42E+05	6.69E+03	1.78E-03	7.52E-06	0.133139	0.997503	**0.5**
AF113-9	**4337 ± 72**	3.22E+05	5.18E+03	1.40E-03	5.91E-06	0.098284	0.998448	**0.4**
AF113-10	**1237 ± 23**	1.73E+05	2.44E+03	2.14E-04	2.62E-06	0.04931	0.999683	**1.5**
AF113-11	**1778 ± 37**	4.33E+05	7.71E+03	7.70E-04	8.03E-06	0.308089	0.996736	**1.1**
AF113-12	**570 ± 14**	9.04E+05	1.22E+04	5.15E-04	1.06E-05	0.406014	0.993343	**3.3**
AF113-13	**2853 ± 68**	1.13E+05	2.51E+03	3.22E-04	2.76E-06	0.05149	0.999657	**0.7**
AF113-14	**1453 ± 24**	1.66E+05	2.21E+03	2.41E-04	2.40E-06	0.017602	0.999742	**1.3**
AF113-15	**1968 ± 50**	2.57E+05	5.68E+03	5.05E-04	6.06E-06	0.181471	0.998227	**1.0**
AF113-16	**2968 ± 62**	2.04E+05	4.03E+03	6.06E-04	4.42E-06	0.129139	0.999084	**0.6**
AF113-17	**1460 ± 22**	2.09E+05	2.53E+03	3.05E-04	2.74E-06	0.040569	0.999659	**1.3**
AF113-18	**1.8 ± 0.1**	7.28E+05	8.87E+03	1.34E-06	1.41E-07	0.044919	0.9989	**1039.4**
AF113-19	**1438 ± 22**	1.65E+05	2.03E+03	2.37E-04	2.21E-06	0.028201	0.999785	**1.3**
AF113-20	**3669 ± 77**	3.81E+05	7.63E+03	1.40E-03	8.52E-06	0.234965	0.996697	**0.5**
AF113-21	**1195 ± 21**	1.72E+05	2.27E+03	2.06E-04	2.45E-06	0.016221	0.999728	**1.6**
AF113-22	**1311 ± 21**	4.01E+05	5.10E+03	5.25E-04	5.34E-06	0.105143	0.998641	**1.4**
AF113-23	**2231 ± 38**	3.01E+05	4.62E+03	6.71E-04	5.01E-06	0.120706	0.998833	**0.8**
AF113-24	**2343 ± 37**	3.73E+05	5.34E+03	8.73E-04	5.83E-06	0.098801	0.998472	**0.8**
AF113-25	**1090 ± 17**	2.14E+05	2.41E+03	2.34E-04	2.60E-06	0.025584	0.999697	**1.7**

Supplementary Table 5 (ST-5): Selected crystal data, data collection and refinement parameters

Crystal data	
Resolution [Å]	42.3-1.90
Space group	$P2_12_12$
No. of protein/RNA per a. u.	1/1
Unit cell *a*, *b*, *c* [Å]	83.66, 139.16, 44.51
Data collection	
No. of unique reflections	40,685
Resolution [Å] (last shell)	1.90 (1.97-1.90)
Completeness [%] (last shell)	96.9 (85.6)
R-merge [%] (last shell)	13.9 (41.7)
Refinement	
R-work/R-free	0.188/0.224
No. of protein and/or RNA atoms	2,860
No. of water molecules	163
No. of Mg^{2+} /Ca^{2+}	1/1
Average B Factors:	
Protein atoms [$Å^2$]	32.5
RNA atoms [$Å^2$]	41.8
Ions / other molecules / water	34.0 / 50.3 / 35.3
R.m.s. deviations:	
Bond lengths [Å]	0.019
Bond angles [°]	2.4
Ramachandran Plot Analysis	274 / 8 / 1
(No. of favored / allowed / outlier)	
Data deposition	
PDB ID	5DO4

Supplementary Figure 3a (SF-3a): SPR imaging analysis of anti-VEGF$_{165}$ aptamer sequence containing a PS2 substitution. The sequence used in this analysis is shown in **ST-1.** The binding curves and K_D corresponding to a global fit are given below. Association was monitored for 200 sec and the dissociation was followed for 500 sec on an EzPlex^{TM} SPRi instrument. The kinetic curves were analyzed using the ScrubberGen software. Reported K_D values are expressed as mean ± SEM, n = 4.

AF83-7

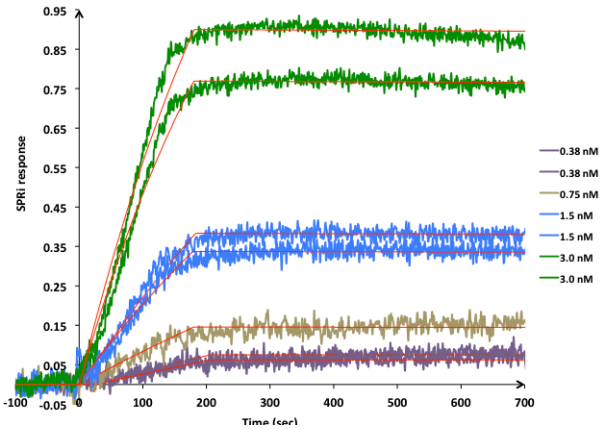

PS2-modified aptamer for VEGF$_{165}$		K_D (pM)
	Aptamer	SPRi
Aptamer obtained from the PS2-walk with a single PS2 substitutions	AF83-7	8.1 ± 0.2

Supplementary Figure 3b (SF-3b): SPR imaging analysis of anti-α-thrombin aptamer sequence containing a PS2 substitution. The aptamer sequence used in this analysis is shown in **ST-2.** The binding curves and K_D corresponding to a global fit are given below. Association was monitored for 200 sec and the dissociation was followed for 500 sec on an EzPlex™ SPRi instrument. The kinetic curves were analyzed using the ScrubberGen software. Reported K_D values are expressed as mean ± SEM, n = 4.

AF113-18

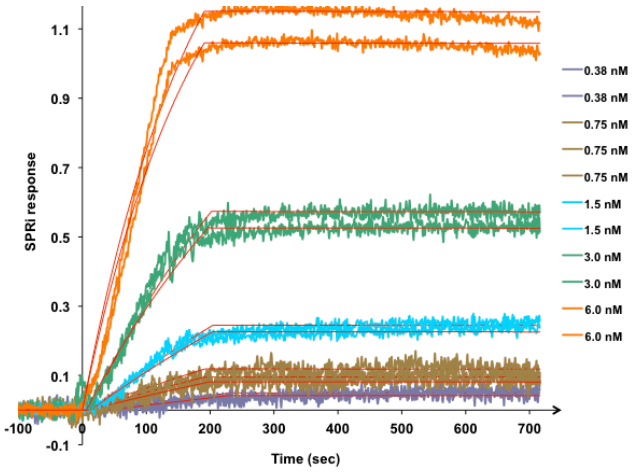

PS2-modified aptamer for α-thrombin		K_D (pM)
	Aptamer	SPRi
Aptamer obtained from the PS2-walk with a single PS2 substitutions	AF113-18	4.5 ± 0.2

Supplementary Figure 4 (SF-4): Circular dichroism spectra of AF83-7 and AF113-18 with their native aptamers AF83-1 and AF113-1, respectively.

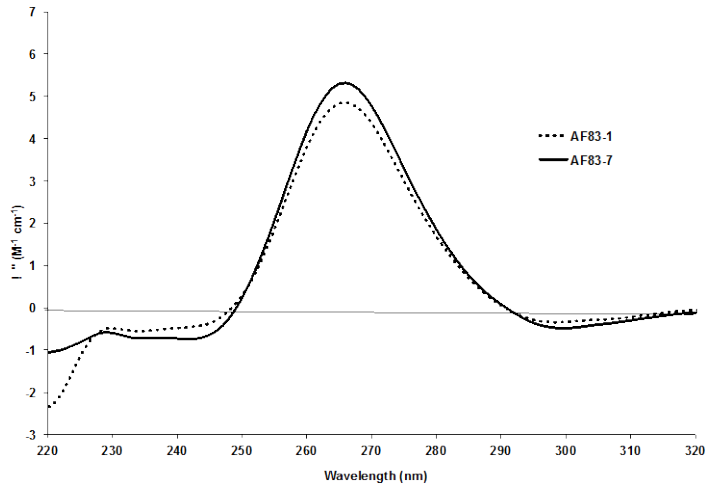

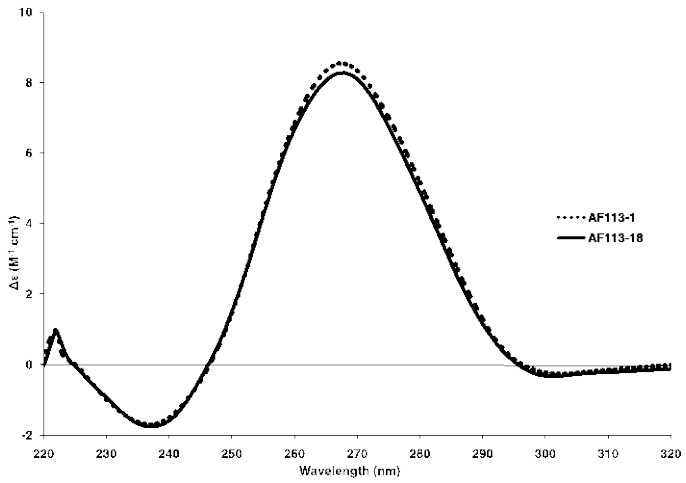

Supplementary Figure 5 (SF-5): Specificity of PS2-modified aptamers

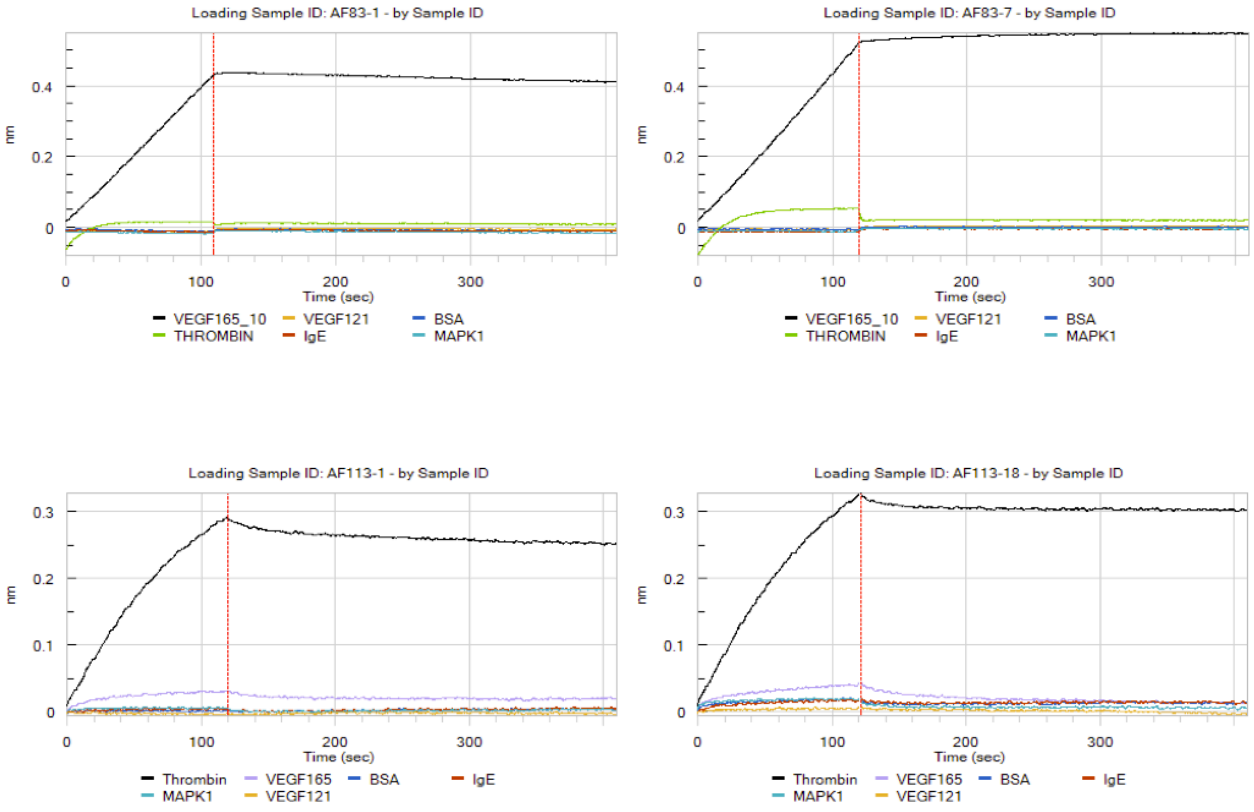

Supplementary Figure (SF-6): Stability of anti-VEGF$_{165}$ aptamers in human serum *in vitro*

The percentage of intact aptamer was calculated as the percent ratio of band intensity = (band intensity at time t ÷ band intensity at 0 h) × 100%. The following is a representation of three independent experiments. We also included Macugen (sequence below) as a reference.

Macugen sequence

5'-$C_FG_{OMe}G_{OMe}AAU_FC_FA_{OMe}G_{OMe}U_FG_{OMe}A_{OMe}A_{OMe}U_FG_{OMe}C_FU_FU_FA_{OMe}U_FA_{OMe}C_FA_{OMe}U_FC_FC_FG_{OMe}$T-3'

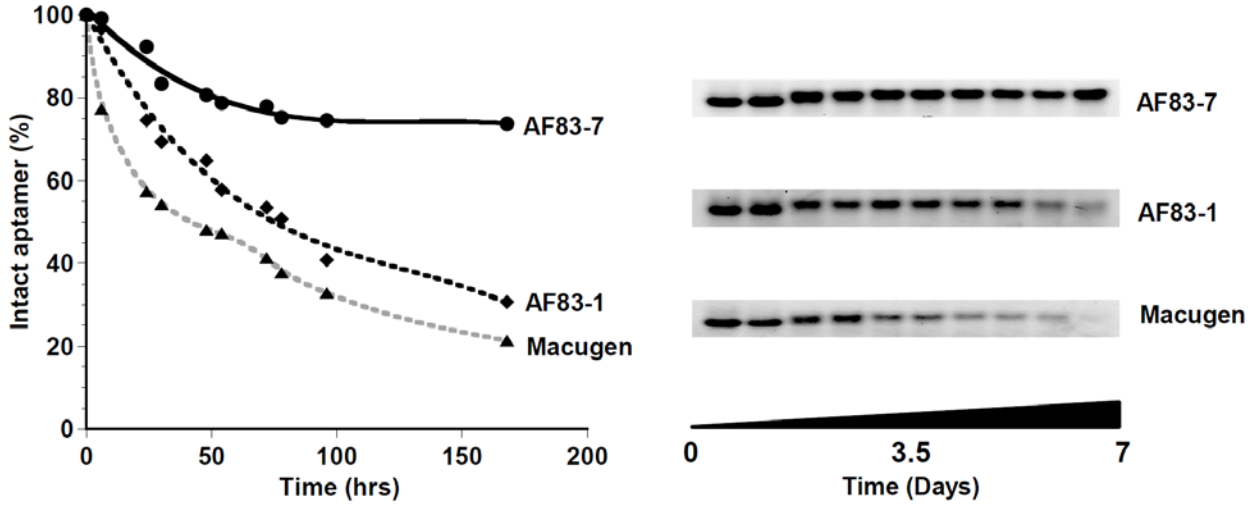

Supplementary Figure 7 (SF-7): The hydrophobic pocket on the surface of thrombin harboring the phosphorodithioate group between U17 and A18. (A) Surface diagram in the region of the pocket, with Phe232 forming the floor and Arg126, Arg233, Lys235 and Lys236 forming the walls. Patches of low and high hydrophobicity are indicated in purple and green, respectively. (B) The PS2 moiety lodged in the hydrophobic pocket depicted in panel A. Thin lines indicate interactions between PS2 sulfur atoms and thrombin Phe232 and the aliphatic portion of the Arg126 side chain as well as RNA A7 and G16.

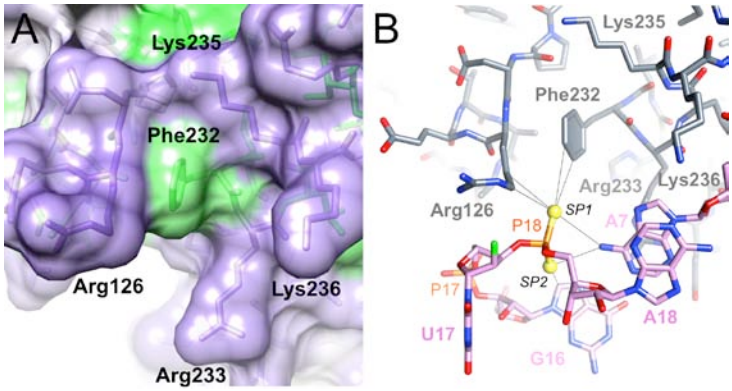

Supplementary Figure 8 (SF-8): The effect of substituting the PS2 with a PSO in AF83-7. Relative K_D values are obtained by dividing the K_D of the select aptamer ($K_D^{AF83\text{-}1}$) by that of the PS2-modified residue containing aptamer ($K_D^{AF83\text{-}7}$).

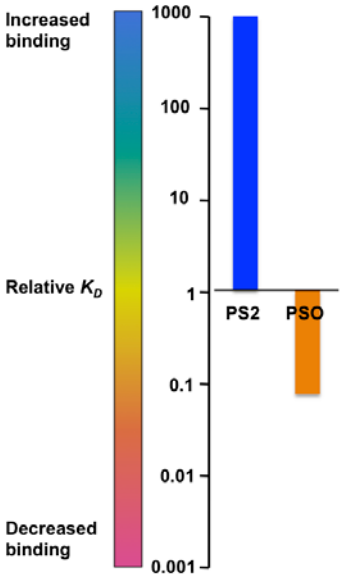

Supplementary Figure 9 (SF-9): The effect of substituting the PS2 with a PSO in AF113-18. Relative K_D values are obtained by dividing the K_D of the select aptamer ($K_D^{AF113\text{-}1}$) by that of the PS2-modified residue containing aptamer ($K_D^{AF113\text{-}18}$).

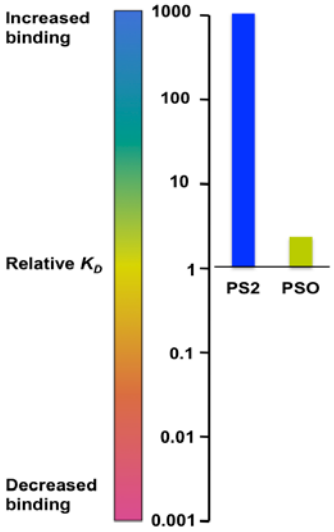

Supplementary Figure 10 (SF-10): Overall views of the AF113-18 PS2-modified RNA:α-thrombin complex. For crystallization experiments, we used human thrombin that was covalently modified with the protease inhibitor D-Phe-Pro-Arg chloromethylketone (PPACK) in order to minimize proteolysis. Co-crystals of thrombin in complex with the 25 nucleotide-long FPS2-modified AF113-18 RNA aptamer

diffracted to 1.9 Å resolution. Electron density maps generated from initial phases obtained by molecular replacement using α-thrombin without RNA from the crystal structure of the native complex (PDB ID code 3DD2) readily revealed the aptamer and positive difference electron density around the 2′-substituent of two 2′-SeMe-modified ribonucleotides confirmed the correct orientation of the aptamer. Selected crystal data, X-ray data collection, and refinement statistics are listed in **Supplementary Table 5**. The final model contains the entire 25-nucleotide aptamer, thrombin light-chain (L) residues 4L through 36L and heavy-chain (H) residues 1H through 258H, the PPACK inhibitor, 163 water molecules, and one magnesium and one calcium ion. In addition, Asn-53 was found to be modified with an N-acetyl-D-glucosamine moiety. Overall views of the aptamer-thrombin complex are depicted in here.